IOP Conf. Series: Materials Science and Engineering **251** (2017) 012128 doi:10.1088/1757-899X/251/1/012128

Numerical study of Tallinn storm-water system flooding conditions using CFD simulations of multi-phase flow in a large-scale inverted siphon

K Kaur[1], **J Laanearu**[1] **and I Annus**[1]

[1]Department of Civil Engineering and Architecture, School of Engineering, Tallinn University of Technology, Tallinn, 19086, Estonia

E-mail: katrin.kaur@ttu.ee

Abstract. The numerical experiments are carried out for qualitative and quantitative interpretation of a multi-phase flow processes associated with malfunctioning of the Tallinn storm-water system during rain storms. The investigations are focused on the single-line inverted siphon, which is used as under-road connection of pipes of the storm-water system under interest. A multi-phase flow solver of Computational Fluid Dynamics software OpenFOAM is used for simulating the three-phase flow dynamics in the hydraulic system. The CFD simulations are performed with different inflow rates under same initial conditions. The computational results are compared essentially in two cases 1) design flow rate and 2) larger flow rate, for emptying the initially filled inverted siphon from a slurry-fluid. The larger flow-rate situations are under particular interest to detected possible flooding. In this regard, it is anticipated that the CFD solutions provide an important insight to functioning of inverted siphon under a restricted water-flow conditions at simultaneous presence of air and slurry-fluid.

1. Introduction

Flooding in urban areas is a serious hazard that can obstruct functioning of the public services due to breakdown of city transport, cutoff of electricity, etc. The storm-water system can experience considerable changes in flow, which can range from large volumetric flows during intense rains to longer periods of much smaller flows. The sediments such as sand, mud, etc. depositions take place in the storm-water system, and a multi-phase flow may develop at depressions under certain circumstances. Sediments deposition can generate problems such as hydraulic overloading due to a reduction in flow capacity, which may result in flooding during a storm event. Thus, the issue of designing storm-water systems to be self-cleaning becomes very important. Hou et al. [1] and Laanearu et al. [2] have demonstrated experimentally that the presence of air inside water column can significantly modify the flow dynamics during filling and emptying of large-scale pipeline, respectively. Water-column mass changes during two-phase flow are theoretically analyzed and parameterized in Laanearu et al. [3] [4]. According to Hou et al. [5], rapid filling of an empty pipeline with undulating elevation profile can occur under gravity and if the generated flow is not seriously blocked, the water column grows with little adverse pressure and can attain a high velocity. According to Laanearu et al. [2], emptying of initially filled pipeline is associated with stratified flow due to development of air cavity. Apparently, the presence of heavier substances in the pipeline in addition to air may considerably change the water-flow

Content from this work may be used under the terms of the Creative Commons Attribution 3.0 licence. Any further distribution of this work must maintain attribution to the author(s) and the title of the work, journal citation and DOI.
Published under licence by IOP Publishing Ltd

dynamics e.g. due to the propensity of sediments depositions. Therefore, sand traps are used to reduce sand amount in the storm-water system. Nabil et al. [6] demonstrated that there is a satisfactory agreement between CFD simulation results of slurry-fluid flow and experimental data in case of fine slurries. In the preliminary study of Kaur et al. [7], several CFD simulations were used to determine two-phase flow dynamics in a large-scale storm-water system part i.e. the inverted siphon also under interest in the present study. In latter study two cases: 1) rapid filling of the system containing a stagnant water at constant water inflow rates, and 2) emptying the initially, partially filled system from slurry-fluid at constant inflow rates of water, were investigated. Instead of the steady hydraulically-driven flows, the computational results revealed unexpected unsteady two-phase flow situations with the design flow rates (air and water: 1000 lps and less). When the driving pressure-head was high, which is associated with an ascending water level in the inlet chamber of siphon, air from the inverted siphon was effectively expelled out, after which the flow was accelerated, and if the water level in the inlet chamber was descending below the upper invert of siphon then the air intake occurred. Apparently quasi-stationary pressure oscillations in the inverted siphon are a cause of this phenomenon, where the air-water-flow stage is replaced with water-flow stage and vice versa with a characteristic period.

Until present the restricted water-flow conditions in the Tallinn storm-water system due to simultaneous presence of air and sediments have been poorly examined. To investigate the three-phase flow dynamics in the storm-water system, more advanced numerical study of a restricted water flow through the large-scale inverted siphon is herein conducted. In addition of three phases of flow also the inverted-siphon walls representation in the CFD solutions is modified. For this purpose a rough-wall function is activated in the applied multi-phase flow solver to better simulate realistic conditions. An aim of the present study is to determine flooding conditions in the case of emptying the initially, partially filled inverted siphon from slurry-fluid at constant inflow rates of water. It is anticipated that the presence of slurry-fluid in the inverted siphon reduces the flow capacity, and modifies significantly the water-flow dynamics through the inverted siphon as compared by the previous results by Kaur et al. [7].

The plan of the current study is following. Firstly the CFD solver structure is briefly presented. The numerical simulations are investigated for two cases: 1) designed flow rate and 2) larger flow rate, for emptying the initially filled inverted siphon from slurry-fluid. Specifically, the case (2) is presented in two stages to detected flooding. For consistency check the stationary flow conditions in the numerical simulations are compared with the hydraulic results. Finally the overall results are discussed and concluded.

2. CFD solver setup

2.1. Inverted siphon

The hydraulic system (figure 1) consists of two reinforced-concrete chambers at inlet and outlet, which both include a manhole on top. The inlet and outlet chambers at sides are equipped with inflow and outflow pipes, respectively. The inlet and outlet chambers are connected by the siphoned part, consisting of pipeline with the inner diameter of 800 mm and the length of 90 m. The inverted siphon is constructed from centrifugally cast fiberglass-reinforced, polymer mortar pipes, which is characterized with an approximate Manning's roughness coefficient n = 0.015. The reinforced-concrete chambers have dimensions of 1.5 m × 2.0 m × 3.0 m. The siphoned part consists of three sections: inflow pipe with a positive slope i_0 = 0.327 and length l = 13.3 m, the middle section at the lowest part with a minor positive slope i_0 = 0.001 and l = 55.3 m and outflow pipe with the adverse slope i_0 = -0.157 and l = 21.2 m. Extra pipe connections are designed at the lowest pipe of siphon for maintenance purposes. In this regard, the use of flushing devices that generate controlled flush waves into the system are considered as a possible solution to remove the flow-restricting substances from the lower part of the inverted siphon. The designed flow rate of the system is 1000 lps. Hydraulic modelling of fully filled steady-state flow to determine head losses, hydraulic gradients and wall shear stresses at Reynolds numbers in the expected operational range is presented by Kaur et al. [7].

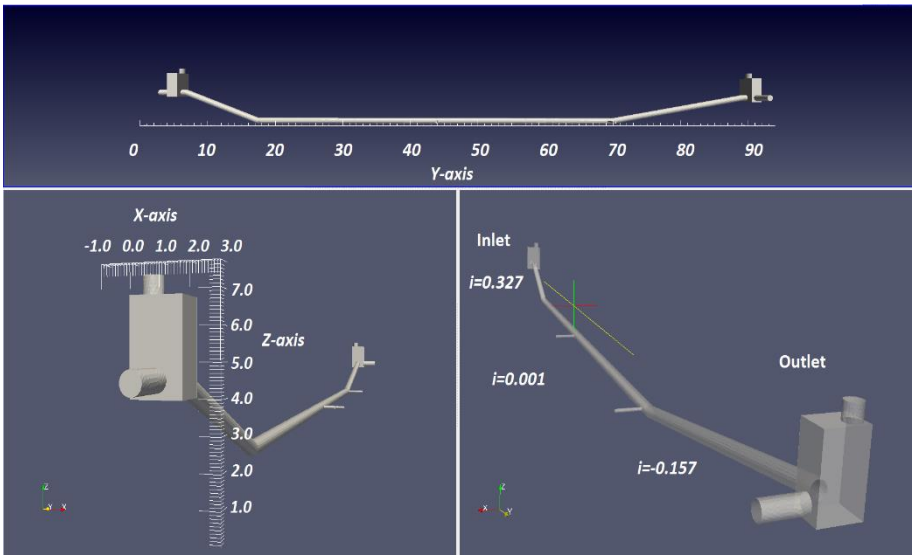


Figure 1. Full-scale CAD model of the inverted siphon under Laagna Road.

2.2. Multi-phase flow solver

A multi-phase flow solver of Computational Fluid Dynamics software OpenFOAM for a number of fluids is used. The solver includes surface-tension and contact-angle effects for each phase. The numerical technique used in the CFD modelling is the Volume of Fluid (VOF) method. A pressure-based solver considering the relationship between velocity and pressure corrections, following mass conservation and momentum changes is used. Convergence can be obtained by progressively tracking the imbalances in numerical calculations of algebraic equations, through each iteration step. These imbalances measure the overall conservation of residuals and convergence solutions can be achieved when these residuals are reduced under pre-set tolerances. In the processing step, the flow variables such as velocity, pressure and density are approximated by means of simple functions. In the post-processing step these variables are visualized.

A full scale three dimensional model of the inverted siphon (figure 1) is constructed and meshed in the pre-processing phase. Also, in this phase, fluid, pipe wall material and turbulence properties are defined and initial and boundary conditions are selected. Fields are set to clearly define the initial distribution of fluids: water at the inflow, slurry-fluid in the bottom of the inverted siphon as a stagnant pool up to a level that represents real-life conditions, and air, as default, everywhere else in the computational domain.

In the processing step a solver for *n* incompressible fluids is implemented for the three-phase flow of interest in this study. At appropriate boundaries of the computational domain wall-function for turbulent flow over rough walls is applied. The roughness parameter for the wall shear stress in this model is defined via equivalent sand-grain roughness, which can be calculated from the Darcy friction factor by a relation defined by Adams et al. [8]:

$$k_s = 3.7D\left(10^{-\frac{1}{1.8\sqrt{\lambda}}} - \frac{6.9}{Re}\right)^{1/1.11} \quad (1)$$

where D is the pipe diameter in meters, λ is the friction factor (set to 0.03) as the flow is operated in a fully turbulent regime, and Re is the Reynolds number.

2.2.1. Volume of Fluid method. The multi-phase flow solver is based on the VOF method and calculates a multiphase mixture that is used to find physical properties as weighted averages based on phase fraction α_q that can take any value between 0 and 1.

The VOF method can be classified as a Surface Capturing technique which implies that the free-surface is not exactly tracked by the mesh like in Surface Tracking methods, but its position is approximated by a phase fraction function [9]. The momentum equation

$$\frac{\partial}{\partial t}(\rho_m \vec{u}) + \vec{\nabla}\cdot(\rho_m \vec{u} \otimes \vec{u}) = -\vec{\nabla} p_{rgh} + \vec{\nabla}\cdot\left[\mu_m(\vec{\nabla}\vec{u} + \vec{\nabla}\vec{u}^T)\right] - (\vec{g}\cdot\vec{x})\vec{\nabla}\rho_m + \sigma\kappa\vec{\nabla}\alpha_q \quad (2)$$

The continuity equation

$$\vec{\nabla}\cdot\vec{u} = 0 \quad (3)$$

The phase fraction α_q for a phase-pair can be computed from a separate transport equation that takes the form

$$\frac{\partial \alpha_q}{\partial t} + \vec{\nabla}\cdot(\alpha_q \vec{u}) = 0 \quad (4)$$

To achieve the necessary compression of the surface an extra artificial compression term is introduced into the latter equation

$$\frac{\partial \alpha_q}{\partial t} + \vec{\nabla}\cdot(\alpha_q \vec{u}) + \vec{\nabla}\cdot\left[\alpha_q(1-\alpha_q)\vec{v}_{qp}\right] = 0 \quad (5)$$

where $\vec{v}_{qp}$ is a velocity field suitable to compress the interface. This artificial term is only active in the interface region.

The density at any point in the domain is calculated as a weighted average of the volume fraction

$$\rho_m = \alpha_q \rho_i + (1-\alpha_q)\rho_j \quad (6)$$

The curvature κ in the momentum equations surface tension term $\vec{F}_\sigma = \sigma\kappa\vec{\nabla}\alpha_q$ is given by equation

$$\kappa = \vec{\nabla}\cdot\left(\frac{\vec{\nabla}\alpha_q}{|\vec{\nabla}\alpha_q|}\right) \quad (7)$$

The treatment of the pressure is done using modified pressure p_{rgh} that is related to the pressure gradient via the equation

$$-\vec{\nabla}p + \rho_m \vec{g} = -\vec{\nabla}p_{rgh} - (\vec{g}\cdot\vec{x})\vec{\nabla}\rho_m \quad (8)$$

where $\vec{x}$ is the position vector.

2.2.2. Turbulence model. The standard k-ε model of Jones and Launder [10], based on Boussinesq approximation with the turbulent viscosity μ_t is used in the multiphase solver. The turbulent viscosity equation is

$$\mu_t = \rho C_\mu \frac{k^2}{\varepsilon} \quad (9)$$

The transport equation for turbulent kinetic energy k, that determines the energy in the turbulence, takes the form

$$\frac{\partial}{\partial t}(\rho k) + \frac{\partial}{\partial x_i}(\rho k u_i) = \frac{\partial}{\partial x_j}\left[\left(\mu + \frac{\mu_t}{\sigma_k}\right)\frac{\partial k}{\partial x_j}\right] + P_k + P_b - \rho\varepsilon - Y_M + S_k \quad (10)$$

The transport equation for turbulent dissipation ε, that determines the scale of the turbulence, takes the form

$$\frac{\partial}{\partial t}(\rho\varepsilon) + \frac{\partial}{\partial x_i}(\rho\varepsilon u_i) = \frac{\partial}{\partial x_j}\left[\left(\mu + \frac{\mu_t}{\sigma_\varepsilon}\right)\frac{\partial \varepsilon}{\partial x_j}\right] + C_{1\varepsilon}\frac{\varepsilon}{k}(P_k + C_{3\varepsilon}P_b) - C_{2\varepsilon}\rho\frac{\varepsilon^2}{k} + S_\varepsilon \quad (11)$$

where the model constants are assigned the following standard values:

$$C_{1\varepsilon} = 1.44, C_{2\varepsilon} = 1.92, C_{3\varepsilon} = -0.33, C_\mu = 0.09, \sigma_k = 1.0, \sigma_\varepsilon = 1.3$$

Also, a boundary condition is provided for turbulent kinematic viscosity for rough walls, based on turbulence kinetic energy. This condition manipulates a parameter to account for roughness effects. The modified law of the wall that incorporates surface roughness, proposed by Cebecci and Bradshaw [11], based on sand-grain mean roughness height k_s takes the form:

$$u^+ = \frac{1}{K}\ln(y^+) + B - \Delta B(k_s^+) \quad (12)$$

where ΔB is a roughness function of $k_s^+ = {k_s u_\tau}/{\nu}$ based on experimental data, B=5.2, and K is von Karman's constant.

3. Case study

In the Tallinn city areas under interest the functioning of storm-water system during intense rains can yield floods. The aim of CFD simulations herein is to investigate a restricted water flow through the siphon with presence of air and slurry-fluid simultaneously. The geometry of the inverted siphon is constructed using a standard CAD software, and the computational domain is meshed with over 100'000 cells.

3.1. Three-phase flow simulations

To determine flooding conditions, the CFD simulations are performed for five different cases, which correspond to flow rates 500, 1000, 1500, 2000 and 3000 lps. All numerical experiments are conducted under same initial conditions, where the inverted siphon is initially partially filled with slurry-fluid up to a level of 2 meters from the lowest part of the pipe, which is determined appropriate to simulate real conditions of the storm-water system. The overall dynamics of different cases is found to be similar, and therefore the computational results are essentially compared for two cases 1) designed inflow rate: 1000 lps and 2) large inflow rate: 2000 lps, for emptying the initially filled inverted siphon from slurry-fluid. Lasting inflows of water into the partially slurry-fluid filled inverted siphon are simulated until the stationary flow conditions are reached.

The density and viscosity of water is 1000 kg/m^3 and 1.0×10^{-6} m^2/s, respectively, and for air is 1.2 kg/m^3 and 1.5×10^{-5} m^2/s, respectively. According to Engineering ToolBox the density and viscosity of slurry-fluid is 1200 kg/m^3 and 1.0×10^{-6} m^2/s, respectively. Fluids in the numerical modelling are considered incompressible and immiscible.

3.1.1. Design flow rate. To investigate a restricted water flow patterns, which correspond to designed flow rate, the numerical test is conducted for 1000 lps. As expected, the siphon is self-cleaning at the designed flow rate, and during the simulation no flooding occurs. The numerical solution reveals a steady-state fully filled pipe flow during the iteration period of 300 000 steps. The steady flow through the siphon in the inflow chamber is characterized with the water level 5.7 m from the reference level, which corresponds to the lowest point of the inverted siphon, and the corresponding pressure-head drop is 1.25 m (figure 2). The corresponding Darcy friction factor $\lambda = 0.0551$ and Reynolds number $Re = 1.5915 \times 10^6$.

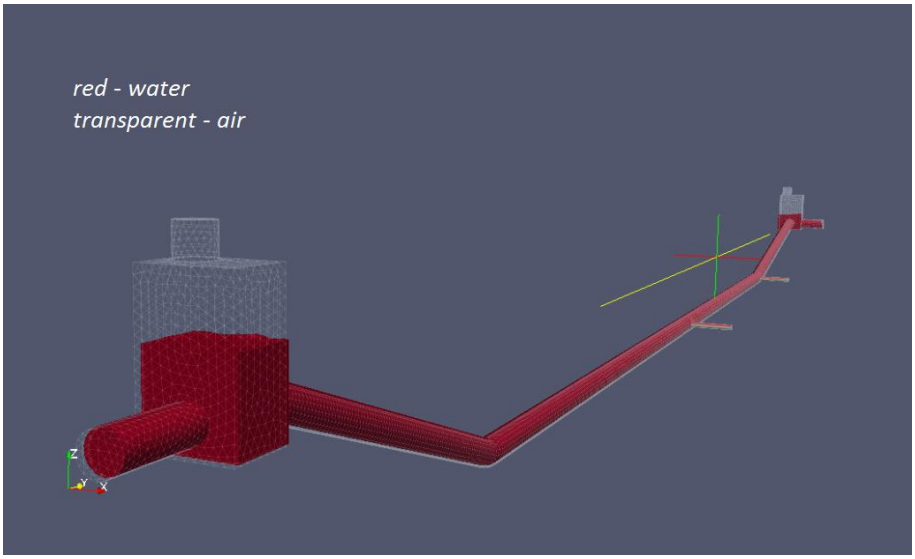


Figure 2. A CFD solution for design flow rate: steady flow stage.

3.1.2. Larger flow rate. The numerical test is conducted for 2000 lps, which correspond to the larger flow rate as compared to the designed flow rate. Now a restricted water flow patterns reveals more complicated dynamics. Initially the three-phase flow develops inside the inverted siphon and also the water outflow occurs from the manhole of concrete chamber. The unsteady two-phase flow for the larger flow rate is temporally associated with presence of flooding. After removal of the slurry-fluid from the inverted siphon i.e. in the final stage, the flow reveals the stationary flow conditions with the increased water level in the inlet concrete chamber, and the increased pressure drop as compared to the numerical test with the designed flow rate.

3.1.2.1 *Unsteady flow stage.* The computational results initially reveal that the unsteady three-phase flow situation causes the increasing pressure-head, which is associated with an ascending water level in the inlet chamber of the inverted siphon. Before the slurry-fluid is expelled out from the inverted siphon, the water level is reaching to the outlet level of the inlet chamber manhole (figure 3). Apparently the increased pressure-gradient due to mixed fluids in the inverted siphon are a cause of this phenomenon. Thus initially, before the slurry-fluid is being flushed out by water inflow, flooding occurs. It can be concluded that during the initial period of unsteady flow, the hydraulic gradient is significantly increased, and until self-cleaning occurs, the pressure in the inlet chamber is large enough to produce flooding.

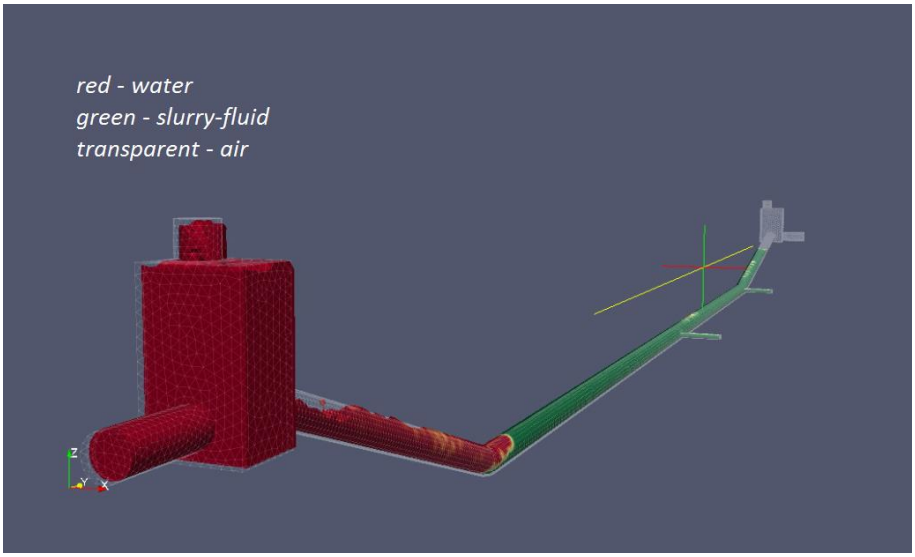


Figure 3. A CFD solution for larger flow rate: unsteady flow stage.

3.1.2.2 *Steady flow stage.* After the initial period of unsteady flow, when the self-cleaning occurs, the computational results reveal that the unsteady flow situation causes the decreasing pressure-head, which is associated with a descending water level in the inlet chamber of siphon. After the slurry-fluid is effectively expelled out from the inverted siphon, the water level is descending below the outlet level of the inlet chamber manhole. The numerical solution reveals a steady-state fully filled pipe flow during the iteration period of 300 000 steps. The steady flow through the siphon in the inflow chamber is characterized with the water level 7.0 m from the reference level, which corresponds to the lowest point of the inverted siphon, and the corresponding pressure-head drop is 2.2 m (figure 4). The corresponding Darcy friction factor $\lambda = 0.0242$ and Reynolds number $Re = 3.1831 \times 10^6$.

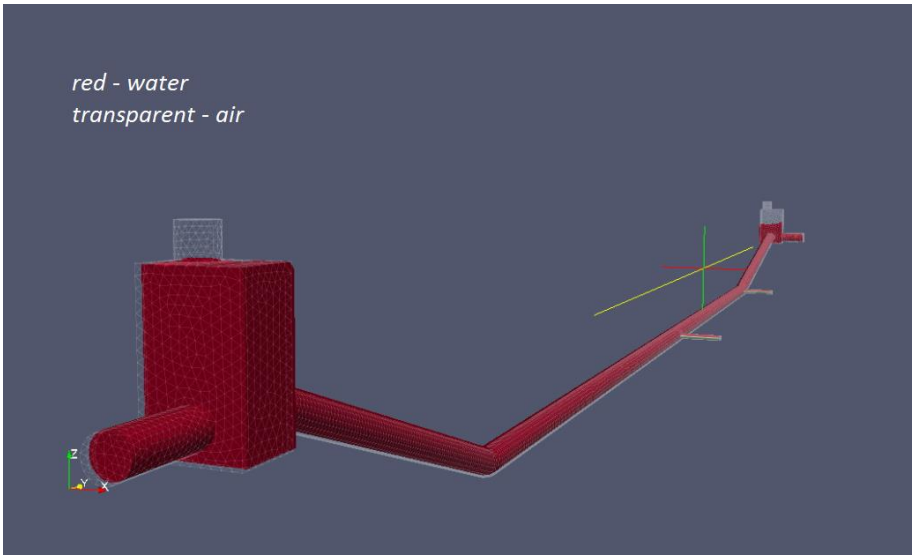


Figure 4. A CFD solution for larger flow rate: steady flow stage.

4. Conclusions and discussion

CFD solutions are used to determine the two- and three-phase flow dynamics in the large-scale inverted siphon, which is part of the storm-water system under road in Tallinn. The initially slurry-fluid filled inverted siphon flushing with water is investigated to find flooding conditions. The computational results demonstrate that no flooding occurs at flow rates smaller than 2000 lps even when the slurry-fluid is present in the system. Flooding does occur at 2000 lps at the inlet chamber in the computational phase where the slurry-fluid is still being flushed out and resides when it is discharged and fully-filled steady state pipe water flow develops.

An interesting result that is not presented above, but definitely merits discussion and further investigation is a simulation result at a small flow rate of 500 lps. In that case free surface flow is observed and a steady hydraulic jump seemingly occurs at the approximate height of 3.8 m with a zero level at the lowest part of siphoned part.

The next step of the investigation will be to use the extensive capabilities of CFD solvers and increase computational accuracy with dynamic meshing. Another step is to experimentally specify turbulence model constants for multi-phase flow. It would be also of interest to conduct experiments for different slurry fluid properties in addition to the here considered fine slurry, that can be modelled as a Newtonian fluid. Uncertainty of hydraulic resistance was estimated to be 0.02 and therefore, the hydraulic verification of the numerical boundary functions need more attention in any future work.

Acknowledgments

This work is supported by institutional research funding IUT (19-17) of the Estonian Ministry of Education and Research. Authors would like to express their sincere gratitude to Malle Ütt from Engineering and consultancy company K-projekt, and Margus Koor from Water company AS Tallinna Vesi for their help and the technical data of the storm-water system in Tallinn.

References

[1] Hou Q, Tijsseling A S, Laanearu J, Annus I, Koppel T, Bergant A, Vučković S, Anderson A and Van ’t Westende J M C 2014 Experimental investigation on rapid filling of a large-scale pipeline *ASCE J. Hyd. Eng.* **140** (11), 1−14

[2] Laanearu J, Annus I, Koppel T, Bergant A, Vučković S, Hou Q, Tijsseling A S, Anderson A and van ’t Westende J M C 2012 Emptying of large-scale pipeline by pressurized air *ASCE J. Hyd. Eng.* **138** (12), 1090−100

[3] Laanearu J, Hou Q and Tijsseling A S 2015 Experimental and analytical modelling study of water-front dynamics of two-phase unsteady flows in a large-scale pressurized pipeline *12th Int. Conf. on Press. Surg., Fluid Trans. and Water Hammer* pp 625−637
[4] Laanearu J, Hou Q, Annus I and Tijsseling A S 2015 Water-column mass losses during the emptying of a large-scale pipeline by pressurized air *Proc. Estonian Acad. Sci.* **64**(1), 8–16
[5] Hou Q, Zhang L X, Tijsseling A S and Kruisbrink A C H 2011 Rapid filling of pipelines with SPH particle method *Proc. Eng.* **31**, 38-43
[6] Nabil T, El-Sawaf I and El-Nahhas K 2014 Sand-water slurry flow modelling in a horizontal pipeline by computational fluid dynamics technique *Int. Water Tech. J.* **4**(1)
[7] Kaur K, Laanearu J and Annus I 2016 Using CFD to simulate multiphase flow in a large-scale inverted siphon: Tallinn storm-water system case study *14th Int. CCWI Conf.* (Amsterdam: International Water Conferences)
[8] Adams T, Grant C and Watson H 2012 A Simple Algorithm to Relate Measured Surface Roughness to Equivalent Sand-grain Roughness *Int. J. Mech. Eng. Mech.* **1**(2), 66-71
[9] Carrica P, Wilson R and Stern F 2006 An unsteady single-phase level set method for viscous free surface flows *Int. J. Num. Meth. in Fluids* **53**(2), 229–56
[10] Jones W P and Launder B E 1972 The prediction of laminarization with a two-equation model of turbulence *Int J Heat Mass Transf.* **15**(2), 301–14
[11] Cebeci T and Bradshaw P 1977 *Momentum Transfer in Boundary layers* (New York: Hemisphere Publishing Corporation)